Spectral Evolution of Scorpio X-1 along its Color-Color Diagram

A. D'Aí*, P. Zycki†, T. Di Salvo*, R. Iaria*, G. Lavagetto* and N. R. Robba*

*Dipartimento di Scienze Fisiche ed Astronomiche, Università di Palermo, via Archirafi n.36, 90123 Palermo, Italy.
†CAMK, Bartycka 18, 00-716 Warsaw, Poland

Abstract. We analyze a large collection of RXTE archive data of the bright X-ray source Scorpius X-1 in order to study the broadband spectral evolution of the source for different values of the inferred mass accretion rate by selecting energy spectra from its Color-Color Diagram. We model the spectra with the combination of two absorbed components: a soft thermal component, which can be interpreted as thermal emission from an accretion disk, and a hybrid Comptonization component, which self-consistently includes the Fe Kα fluorescence line and the Compton reflected continuum. The presence of hard emission in Scorpius X-1 has been previously reported, however, without a clear relation with the accretion rate. We show, for the first time, that there exists a common trend in the spectral evolution of the source, where the spectral parameters change in correlation with the position of the source in the CD. Using a hybrid thermal/non-thermal Comptonization model (EQPAIR code), we show that the ratio of the power supplied to the non-thermal distribution to the total power injected into the Comptonizing plasma correlates with the accretion rate, being the highest at the lowest accretion rates. We discuss the physical implications derived from the results of our analysis, with a particular emphasis on the hardest part of the X-ray emission and its possible origin.

Keywords: accretion discs – stars: individual: Scorpio X-1 — stars: neutron stars — X-ray: stars — X-ray: spectrum — X-ray: general
PACS: 97.80.Jp

INTRODUCTION

Scorpius X-1 is the brightest persistent X-ray source in the sky. The X-ray source is an old, low magnetized neutron star (NS), accreting matter transferred through Roche-lobe overflow from a low-mass companion [1]. Scorpius X-1 is a prototype of the class of the Low-Mass X-ray Binaries (LMXBs), and assuming a distance of 2.8 ± 0.3 kpc [2], the source emits close to the theoretical Eddington limit for a 1.4 $M_\odot$ NS ($L_{Edd} \sim 2 \times 10^{38}$ erg s^{-1}). Based on the timing behavior of LMXBs in correlation with the position of a given source in the X-ray color-color diagram (CD), Hasinger and van der Klis [3] grouped these sources into two categories: the Z sources and the Atoll sources. The former are brighter, radiating close to L_{Edd}, while the latter emit at 0.01–0.1 L_{Edd}. Z sources exhibit the classical three-shaped branches describing a Z pattern in the CD: the Horizontal Branch (HB) at the top of the Z track, followed by the Normal Branch (NB) and the Flaring Branch (FB) at the bottom of the pattern. There are strong indications [4] suggesting that what drives the changing in the spectral and temporal properties of LMXBs is the instantaneous accretion rate ($\dot{M}$), which, for Z sources, is

CP924, *The Multicolored Landscape of Compact Objects and their Explosive Origins - Cefalù 2006,*
edited by T. Di Salvo, L. A. Antonelli, G. L. Israel, L. Piersanti, A. Tornambè, L. Burderi, F. Fiore, G. Matt, and M. T. Menna

believed to increase monotonically from the HB to the FB. Spectral studies of Scorpius X-1 have been so far not so extensive and detailed as timing studies. This is in part due to the strong brightness of the source that actually prevents its observation with the most sophisticated and high-resolution X-ray satellites. Satellites provided with proportional counters have so far given the most reliable spectra of this source; in particular, thanks to its large effective area and broadband energy range (3-200 keV), the still operating RXTE satellite has performed the best X-ray broadband observations.

In this article we report a complete investigation of the spectral properties of Scorpius X-1 through an extensive analysis of RXTE archive data, indicating a clear connection between position of the source on the CD and spectral behavior. In particular we show that the relative strength of hard X-ray emission *is* related to the inferred mass accretion rate; its origin might be explained in the framework of a relativistic non-thermal population of electrons, probably emitted in form of an outflow or collimated jet.

SPECTRAL ANALYSIS

Data reduction and analysis

The scientific payload of RXTE consists of three instruments, the PCA, the HEXTE, and the All Sky Monitor (ASM). The PCA consists of five co-aligned Xenon proportional counter units (PCUs) with a total effective area of about 6500 cm^2. The instrument is sensitive in the energy range from 2 keV up to 60 keV [5], although the response matrix is best calibrated in the energy range 3-32 keV. Data can be processed using several different configuration modes; for our analysis we exclusively use the *Standard2* mode, with 16 s time resolution and 128 energy channels in the 2–60 keV energy range. The HEXTE consists of two cluster of four NaI/CsI-phoswich scintillation counters that are sensitive from 15 keV up to 220 keV [6]. We use the *Standard Mode*, with 64 energy channels, for the reduction and analysis of the HEXTE data. Background subtraction is done by using the source-background rocking of the collimators. We use HEXTE response matrices of 1999 August. We used for our analysis the following datasets: 20035 (1997-04-18 15:20:32 to 1998-01-08 13:19:44), 30036 (1998-01-07 13:29:52 to 1998-01-08 22:16:48) and 40020 (1999-01-06 05:25:20 to 1999-01-16 23:34:40). [1] The total collecting time amounts to $\sim$ 288 ks. Data have been processed using the standard selection criteria, discarding data taken during Earth occultations and passages through the South Atlantic Anomaly. We only used data from PCU2 for the PCA and data from Cluster A for the HEXTE instrument.

We constructed color-color diagrams (CDs) of the source by extracting energy-dependent lightcurves using PCA energy bands 1.94–4.05 keV, 4.05–6.18 keV, 6.18–8.32 keV, 8.32–16.26 keV with a 64 s bin-time. We define the Soft Color (hereafter SC) as the ratio of count rates in the 4.05–6.18 keV and 1.94–4.05 energy bands, while the Hard Color (hereafter HC) as the ratio of count rates in the 8.32–16.26 keV and 6.18–8.32 keV energy ranges. We selected regions in the CDs for each dataset, in order to

[1] In parenthesis we indicated the starting and ending times of the first and last pointed observation in TT.

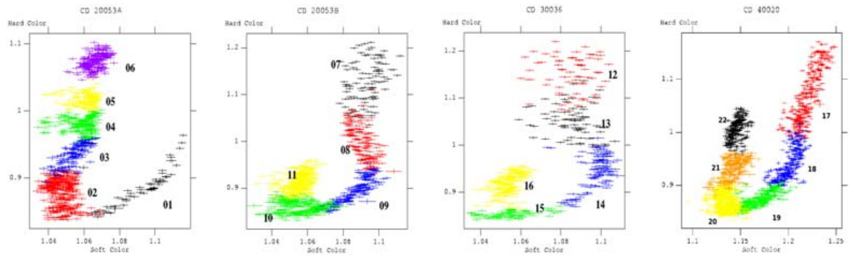

FIGURE 1. CDs extracted from the RXTE datasets used in our spectral analysis. Different colors indicate different selected regions for the energy spectra. We label the spectra through a progressive numbering as shown in the figures.

cover a homogeneous part of the Z-track and to have at the same time a suitable statistics. From these selections we derived the good time intervals (GTI) which we used for extracting the corresponding spectra for the PCA and HEXTE data. We show in Figure 1 the CCDs that we obtained in this way, and the extraction regions for the spectra. Given the high luminosity of the source all the PCA spectra have been dead-time corrected. We have associated an energy dependent systematic error to the PCU2 spectra as follows: 1% up to channels corresponding to an energy lower than 7 keV, 0.5% for channels in the range 7-16 keV, 2% for channels in the energy range 16-22 keV and 5% for channels above 22 keV [7]. No systematic error has been associated to the HEXTE data. A normalization constant is left free to vary between the PCU2 and HEXTE spectra to take into account residual flux calibration uncertainties. Because the PCA energy band starts from 3 keV, it is not possible to constrain the effect of the photoelectric interstellar absorption of the source flux. Following Christian and Swank [8], we fixed its value to 3×10^{21} cm^{-2}, for each fit performed.

We fitted our data with a model given by the sum of a soft `DISKBB` component [9] plus the recently developed thermal/non-thermal hybrid Comptonization model named `EQPAIR` [see 10, for a full description of the model]. This model assumes a spherical plasma cloud with isotropic and homogeneous distribution of photons and $e^{\pm}$, and soft seed photons produced uniformly within the plasma. The properties of the plasma depend on its compactness, $l \equiv \mathscr{L}\sigma_T/(\mathscr{R} m_e c^2)$ where $\mathscr{L}$ is the power of the source, $\mathscr{R}$ is the radius of the sphere and σ_T is the Thomson cross section. The compactness is divided in a hard compactness, l_h, which corresponds to the power supplied to the electrons, and a soft compactness, l_s, corresponding to the power supplied in the form of soft photons. The compactness corresponding to the electron acceleration and to the additional heating of the thermal part of the $e^{\pm}$ distribution are denoted as l_{nth} and l_{th}, respectively, and $l_h \equiv l_{nth} + l_{th}$. The non-thermal energy distribution of the electrons in the plasma is assumed to be a power law; we preliminarily assumed that the power-law replaces the Maxwellian exponential tail from a gamma Lorentz factor $\gamma_{min} = 1.3$ up to a $\gamma_{max} = 1000$ and that its energy index is 2. The fits were generally not sensitive to variations of these parameters so that we fixed these values for all the fits performed. We have left free to vary the following parameters: the soft seed-photon temperature of the Comptonizing cloud kT_0, the optical depth of the cloud τ, l_h/l_s, l_{nth}/l_h and a

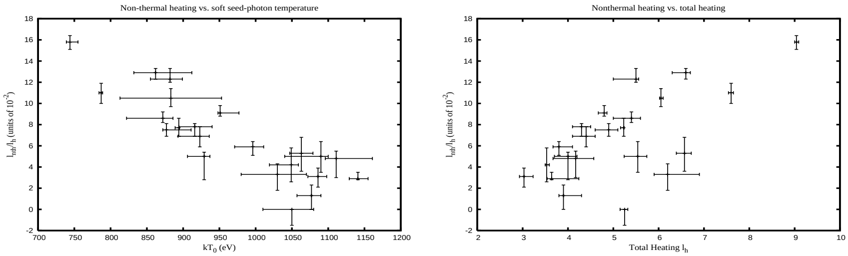

FIGURE 2. Left panel: non-thermal heating fraction (l_{nth}/l_h) versus temperature (kT_0) of the soft seed-photons. Right panel: non-thermal heating fraction versus total heating.

normalization factor. This model contains a self-consistent computation of the reflection component, for which we set as free parameters the reflection amplitude $\Omega/2\pi$, the ionization parameter ξ and also the inner radius of the disk, R_{in} (in units of GM/c^2), which is a measure of the relativistic smearing of the Fe Kα line in proximity of the NS. The value of the soft compactness l_s was unconstrained by the fit (it is mainly driven by the pair production rate, which manifests itself with the annihilation line at energies $\simeq$ 500 keV, obviously far beyond our energy limits), and we set it at the value of 10 [see also 11]. All the other parameters of the model were frozen at the default values.

DISCUSSION AND CONCLUSIONS

We have examined 22 energy spectra of Scorpius X-1 in the 3.0–200 keV energy band using PCA and HEXTE data; the spectra have been extracted from selected regions chosen in the X-ray CD. We produced a CD for each close in time dataset in order to avoid shifts of instrumental origin, and repeated our analysis for each CD obtained in this way, thus having at hand a robust representation of the spectral evolution of the source in all its accretion states. To fit the spectra we adopted a model, which substantially differ from previously adopted modelizations of Z-sources. We interpret the high energy tail of Sco X-1 as a result of a hybrid thermal/non-thermal Comptonization. Adopting this model, we find an adequate description of the spectral behavior of the source for every spectrum in any region of the CD. The values of reduced χ^2 range from 0.37 to 2.01. For 15 spectra we obtained a reduced χ^2 value ≤ 1.0, for 6 spectra the value was below 1.5 and just in one case above. Here we just discuss the main physical spectral characteristics as a whole. An extensive version of these results will be addressed in a forthcoming paper (D'Aí et al. 2007, ApJ, submitted). The soft thermal disk component of the spectrum is dominant only at energies $\leq$ 5 keV, and contributes to less than 10% to the 3–200 keV energy flux, independently of the selected energy spectrum. For this reason the exact shape of the component is poorly constrained by the fits. Using the `DISKBB` component we find that the disk temperature is in the range 0.3-0.6 keV and has a rather large value of the normalization constant (in the range $10^5 - 10^7$). We note that the disk component is mainly driven by residuals in the very low-energy part of the

TABLE 1. SUMMARY OF THE FIT RESULTS WITH THE HYBRID COMPTONIZATION MODEL

Spectral Parameter **Units**	l_h/l_s	kT_0 **keV**	l_{nth}/l_h	τ 10^{-2}
HB	0.65	0.87	11.7	9.8
NB	0.48	0.91	8.4	8.5
bottom FB	0.39	1.08	4.5	8.0
top FB	0.61	1.08	4.7	11.0

spectrum, and could be affected by systematic uncertainties derived by the large photon flux in this band. If we restrict the energy band of our spectra to 3.6-200 keV range, we find that the entire spectrum can be fit by a hybrid Comptonization component, without any need of a softer component. This does not change the best-fitting parameters of the hybrid Comptonization model and we therefore concentrate our discussion on this component.

We summarize in Table 1 the range in which the best-fitting values of the continuum parameters of the EQPAIR component lie for spectra in the same CD position. The soft to hard compactness assumes a wide range of values, driving most of the spectral evolution of the source; because the soft compactness is a frozen parameter, the l_h/l_s ratio gives immediately the power supplied to the plasma electron cloud, which increases from the bottom of the FB to the HB. Spectra taken at the top of the FB are harder ($l_h/l_s \simeq 0.61$) and optically thicker ($\tau \simeq 11$) than any other spectrum observed. This might be related to a different accretion state of the source, which becomes highly super-Eddington. We find that the soft seed-photon temperature of the Comptonization well correlates with the position of the source in the CD, being the highest on the FB and gradually decreasing as the source moves to lower accretion rates. The ratio of the non-thermal to the thermal power supplied to the electron hybrid plasma clearly indicates that the non-thermal component increases as the source moves from high to low accretion rates. Our data description makes immediately clear that the non-thermal contribution depends on the state of the source, being the strongest at lower accretion rates, namely on the HB. This behavior is in agreement with the behavior of the other Z sources [see e.g. 12]. Moreover, this is the first strong detection that a hybrid thermal/non-thermal state smoothly changes according to the accretion state. We present in Fig. 2 two plots that show the link between the broad-band spectral evolution of the source and the behavior of the non-thermal electron distribution. For the 22 examined spectra, when the soft seed photon temperature is plotted versus the fraction of the non-thermal compactness parameter l_{nth}/l_h, there is a clear trend to have higher l_{nth}/l_h values for lower photon temperatures (left panel), while this corresponds to higher values of the total heating luminosity l_h (right panel). The Z source GX 17+2 has also clearly shown a hard tail, when in the right part of its HB, with a ratio $l_{nth}/l_h = 0.11$, but the detection abruptly disappeared when the source moved to higher $\dot{M}$ (Farinelli et al. 13, but see also Di Salvo et al. 14). The amplitude of the reflection component $\Omega/2\pi$ is quite large (average value ~ 1), while the reflecting medium is poorly ionized (ξ generally $\leq$ 100). The R_{in} values (in the range 50-100 R_g) do not show any particular trend with the accretion state and with the other spectral parameters, given also that the parameters describing the amount of reflection have large uncertainties.

A recent INTEGRAL observation of this source (20-200 keV energy range) results in agreement with our results [15], thus confirming the association between position on the CD and hard X-ray behavior. INTEGRAL data seem also to hint to a non-thermal origin of this component, as no high-energy cut-off was present in the spectra that showed the hard-tail. Theoretical spectra and energetic contribution according to the relevant physical parameters involved in the case of a strict coupling with inflow (i.e. accretion to the compact object through the formation of an accretion disk) and outflow (i.e. jets), are a promising way to cover in a self-consistent way all the phases of accretion. An attempt to explicitly compute a jet spectrum, from radio to hard X-rays, has been recently proposed by Markoff et al. [16], where the jet base subsumes the role of the static Comptonizing corona; spectral fits in the case of BH systems (namely Cyg X-1 and GX 339-4) in hard states are consistent with this scenario, but BH soft states and NS systems spectra need yet to be tested in order to understand the limits of validity of the jet model.

REFERENCES

1. D. Steeghs, and J. Casares, *ApJ* **568**, 273–278 (2002).
2. C. F. Bradshaw, E. B. Fomalont, and B. J. Geldzahler, *ApJL* **512**, L121–L124 (1999).
3. G. Hasinger, and M. van der Klis, *A&A* **225**, 79–96 (1989).
4. S. D. Vrtilek, W. Penninx, J. C. Raymond, F. Verbunt, P. Hertz, K. Wood, W. H. G. Lewin, and K. Mitsuda, *ApJ* **376**, 278–288 (1991).
5. K. Jahoda, and PCA Team, *Bulletin of the American Astronomical Society* **28**, 1285–+ (1996).
6. R. E. Rothschild, P. R. Blanco, D. E. Gruber, W. A. Heindl, D. R. MacDonald, D. C. Marsden, M. R. Pelling, L. R. Wayne, and P. L. Hink, *ApJ* **496**, 538–+ (1998).
7. J. Wilms, M. A. Nowak, J. B. Dove, R. P. Fender, and T. di Matteo, *ApJ* **522**, 460–475 (1999).
8. D. J. Christian, and J. H. Swank, *ApJs* **109**, 177–+ (1997).
9. K. Mitsuda, H. Inoue, K. Koyama, K. Makishima, M. Matsuoka, Y. Ogawara, K. Suzuki, Y. Tanaka, N. Shibazaki, and T. Hirano, *PASJ* **36**, 741–759 (1984).
10. P. S. Coppi, “The Physics of Hybrid Thermal/Non-Thermal Plasmas,” in *ASP Conf. Ser. 161: High Energy Processes in Accreting Black Holes*, 1999, p. 375.
11. M. Gierliński, A. A. Zdziarski, J. Poutanen, P. S. Coppi, K. Ebisawa, and W. N. Johnson, *MNRAS* **309**, 496–512 (1999).
12. T. Di Salvo, and L. Stella, *ArXiv: astro-ph/0207219* (2002), `arXiv:astro-ph/0207219`.
13. R. Farinelli, F. Frontera, A. A. Zdziarski, L. Stella, S. N. Zhang, M. van der Klis, N. Masetti, and L. Amati, *A&A* **434**, 25–34 (2005).
14. T. Di Salvo, L. Stella, N. R. Robba, M. van der Klis, L. Burderi, G. L. Israel, J. Homan, S. Campana, F. Frontera, and A. N. Parmar, *ApJL* **544**, L119–L122 (2000).
15. T. Di Salvo, P. Goldoni, L. Stella, M. van der Klis, A. Bazzano, L. Burderi, R. Farinelli, F. Frontera, G. L. Israel, M. Méndez, I. F. Mirabel, N. R. Robba, P. Sizun, P. Ubertini, and W. H. G. Lewin, *ApJL* **649**, L91–L94 (2006), `astro-ph/0608335`.
16. S. Markoff, M. A. Nowak, and J. Wilms, *ApJ* **635**, 1203–1216 (2005).